HYSCORE insights into the distribution of the unpaired spin density in an engineered Cu_A site in azurin and its His120Gly variant

Sergei A. Dikanov,[*,‡] Steven M. Berry,[§,#] Yi Lu[§]

[‡]Department of Veterinary Clinical Medicine, University of Illinois at Urbana-Champaign, Urbana, Illinois 61801, United States

[§]Department of Chemistry, University of Illinois at Urbana-Champaign, Urbana, Illinois 61801, United States

Supporting Information Placeholder

ABSTRACT: A comparative study of the ^1H and ^{14}N hyperfine interactions between the Cu_A site in an engineered Cu_A center in azurin (WT-Cu_AAz) and its His120Gly variant (H120G-Cu_AAz) using the two-dimensional ESEEM technique, HYSCORE, is reported. The HYSCORE spectroscopy has clarified conflicting results in previous EPR and ENDOR studies and found clear differences between the two Cu_A azurins. Specifically, a hyperfine coupling $A_{N\perp}$ = 15.3 MHz was determined for the first time from the frequencies of double quantum transitions of ^{14}N histidine nitrogens coordinated to Cu_A in the WT-Cu_AAz. In contrast, such coupling was not observed in the spectra of H120G-Cu_AAz, indicating at least a several MHz increase of the $A_{N\perp}$ value for the coordinated nitrogen in this variant. In addition, ^{14}N HYSCORE spectra of the WT-Cu_AAz shows interaction with only one type of weakly coupled nitrogen assigned to the remote N_ε of coordinated imidazole residues based on the quadrupole coupling constant ($e^2Qq/4h$) of ~ 0.4 MHz. The spectrum of H120G-Cu_AAz resolves additional features typical for backbone peptide nitrogens with larger $e^2Qq/4h$ of ~ 0.7 MHz. Hyperfine couplings with these nitrogens vary between ~ 0.4-0.7 MHz. In addition, the two resolved cross-peaks from C_β protons in H120G-Cu_AAz displays only ~1 MHz shifts relative to the corresponding peaks in WT-Cu_AAz. These new findings have provided the first experimental evidence for the previous DFT analysis that predicted changes of the delocalized electron spin population of ~0.02-0.03 (i.e. ~10%) on copper and sulfur atoms of the Cu_A center in H120 variants relative to the WT-Cu_AAz and resolved contradicting results between EPR and ENDOR studies of valence distribution in Cu_AAz and its variants.

■ INTRODUCTION

The Cu_A is a binuclear copper center bridged by two cysteine ligands to form a Cu_2S_2 "diamond-core" structure, which has been found naturally in redox enzymes cytochrome *c* oxidase (COX)[1] and nitrous oxide reductase (N_2OR)[2,3] and studied in detail by different spectroscopic techniques.[4-6] The important feature of the Cu_A center is that the two copper ions form a direct metal-metal bond and the unpaired electron is delocalized between two copper ions, and the resting state of the Cu_A center is a Cu(+1.5)−Cu(+1.5) state rather than a Cu(+2)−Cu(+1) state. In addition to the bridging cysteine ligands, the copper ions are coordinated by a histidine from the equatorial position to form a trigonal NS_2 geometry. There is also a weak distal axial ligand on each copper ion, a methionine at one copper and a backbone carbonyl at the other.

The unique structure of the Cu_A site inspired many to design protein models for additional study.[7-10] Hay *et al.* constructed a Cu_A protein from a recombinant T1 copper protein, *Pseudomonas* (*Ps.*) *aeruginosa* azurin, by replacing the loop containing the three ligands to the blue copper center with the corresponding loop of the Cu_A site in COX from *Pa. dentrificans*.[11] The binuclear Cu_A site engineered into *Ps. aeruginosa* azurin, called WT-Cu_AAz hereafter, displayed UV−vis and EPR spectra that were remarkably similar to those of native Cu_A sites in COX from *Pa. dentrificans*. The X-ray crystal structure of WT-Cu_AAz showed a very similar CuSSCu core, with a Cu−Cu distance that was even slightly shorter than the native Cu_A center in COX, confirming the presence of a Cu−Cu bond.[12]

While many studies have focused on elucidating the roles of conserved Cys in the diamond core and the axial ligands[13-16] in fine-tuning the electronic structure and redox properties of the Cu_A center, the role of the equatorial histidine coordinated to each copper ion has not been as well defined. To address this issue, mutations of the equatorial His 120 in Cu_AAz (Scheme 1) to Asn(N) and

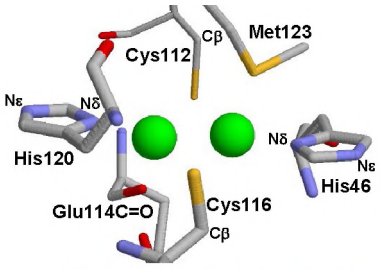

Scheme 1. WT-Cu_A-Az active site (PDB ID: 1cc3)[12]

Gly(G) were made to understand the histidine-related modulation of the valence delocalization over the CuSSCu core.[17,18] Surprisingly, multifrequency (X-, C-, and S-band) electron paramagnetic resonance (EPR) and Q-band electron nuclear double resonance (ENDOR) studies have provided markedly different views of the mutation-induced changes in these two proteins.[19] Multifrequency EPR indicated that the H120N and H120G mutations had changed the hyperfine structure from a 7-line to a 4-line pattern (Figure S1), consistent with trapped-valence, Type 1 mononuclear copper, i.e.

EPR data suggest that the electron spin had become localized on one copper by the His120 mutation. On the other hand, the qualitative (visual) comparison of the Q-band ENDOR spectra led to the conclusion that hyperfine interactions with cysteine C_β protons, weakly dipolar-coupled protons, and the remaining His46 nitrogen ligand were essentially unperturbed by the mutation at His120 implying that the Cu_A core electronic structure was unchanged after the mutation. Orientation selective W-band (95 GHz) ENDOR of cysteine C_β protons in WT-Cu_AAz was also examined in comparison with the several other proteins.[20] However, despite ENDOR studies[19,20] the individual hyperfine couplings of the coordinated histidine nitrogens and cysteine C_β protons in Cu_AAz remains unknown.

To resolve these issues, we report herein our study of WT-Cu_AAz and its His120Gly variant (H120G-Cu_AAz) using the two-dimensional ESEEM technique, called HYSCORE.[21] Similar to ENDOR, HYSCORE provides information about hyperfine interactions with magnetic nuclei ^{1}H and ^{14}N, which are unresolved in CW EPR spectra. Application of HYSCORE spectroscopy has supplemented the data obtained in the ENDOR studies[19,20] and has found clear differences between ^{14}N and ^{1}H hyperfine interactions in wild-type and His120Gly Cu_AAz.

■ EXPERIMENTAL SECTION

Samples. The WT-Cu_AAz and H120G-Cu_AAz were expressed, prepared, and characterized as described elsewhere.[11,17] The concentration of these samples was 1 mM, and they were dissolved in 50% glycerol, 0.1 M phosphate buffer, pH 5.2. EPR spectra of these samples were previously reported.[19]

HYSCORE experiments. Pulsed EPR experiments were carried out at 20 K using an X-band Bruker ELEXSYS E580 spectrometer equipped with an Oxford CF 935 cryostat. Two-dimensional, four-pulse hyperfine sublevel correlation spectroscopy (HYSCORE, $\pi/2$-τ-$\pi/2$-t_1-π-t_2-$\pi/2$-τ-echo)[21] was employed with appropriate phase-cycling schemes to eliminate unwanted features from the experimental echo envelopes. The intensity of the echo after the fourth pulse was measured with t_2 and t_1 varied and constant τ. The length of a $\pi/2$ pulse was nominally 16 ns and a π pulse 32 ns. HYSCORE data were collected in the form of 2D time-domain patterns containing 256×256 points with steps of 16 ns. Spectral processing of ESEEM patterns, including subtraction of the relaxation decay (fitting by polynomials of 3-4 degree), apodization (Hamming window), zero filling, and fast Fourier transformation (FT), was performed using the Bruker WIN-EPR software.

■ RESULTS

Previous CW EPR studies of the samples examined in this work reported that the mixed-valent state of the Cu_A centers in WT-Cu_AAz and H120G-Cu_AAz are characterized by axial ***g*** tensors with principal values $g_\perp$=2.018, $g_\parallel$=2.17 and $g_\perp$= 2.007, $g_\parallel$=2.22, respectively (Figure S1).[19] The two-pulse, echo-detected EPR spectra of WT-Cu_AAz and H120G-Cu_AAz in frozen solutions are shown in Figure S2. The width and location of $g_\perp$ and $g_\parallel$ features in these spectra are consistent with the reported g-tensors.

Strongly coupled nitrogens. The complete presentation of the ^{1}H,^{14}N HYSCORE spectrum of WT-Cu_AAz recorded at the $g_\perp$ area of the EPR signal are shown in Figure 1. The spectrum consists of two quadrants containing cross-peaks from strongly and weakly coupled nitrogens and several protons. The pair of cross-peaks $\mathbf{1}_N$ parallel to the antidiagonal line in the (+–) quadrant (Figure 1a,c) with coordinates of a maximum at (17.0; -12.7) MHz, can be assigned to (dq+; dq-) correlations of strongly coupled ^{14}N, based on their frequency differences being close to $4\nu_{14N}$, their contour lineshape, and their intensities ($dq_\pm$ - double-quantum transitions of ^{14}N nuclear spin I=1 in two opposite m_S manifolds of the electron spin).[22,23] The calculated ^{14}N hyperfine coupling corresponding to these cross-peaks gives the same coupling $A_{N\perp}$=15.3±0.2 MHz using the second-order expression for $\nu_{dq\pm}$ (Eq. 1)[24]

$$A_N = \frac{2\nu_N(\nu_{dq+} + \nu_{dq-})}{8\nu_N - (\nu_{dq+} - \nu_{dq-})} \qquad \text{(Eq. 1)}$$

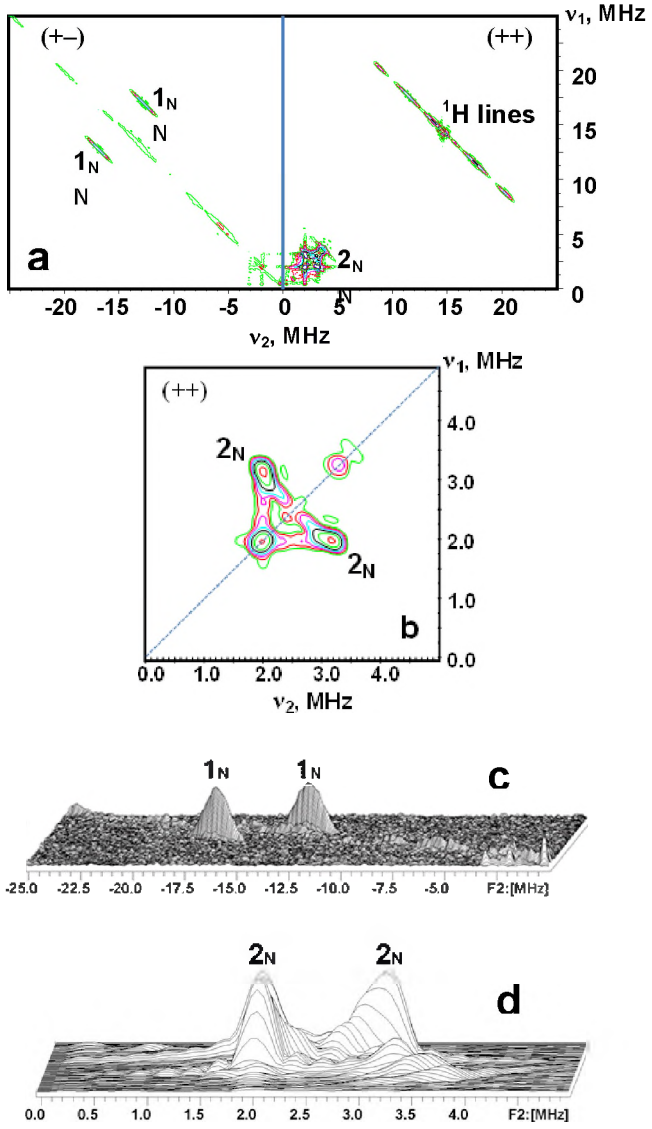

Figure 1. (++) and (+–) quadrants of the ^{1}H and ^{14}N HYSCORE spectrum of WT-Cu_AAz (a) showing location of ^{14}N cross-peaks $\mathbf{1}_N$ and $\mathbf{2}_N$ from strongly and weakly coupled nitrogen nuclei, respectively, and ^{1}H cross-ridges. Cross-peaks $\mathbf{2}_N$ at enhanced resolution are shown in (b). Stacked presentation of cross-peaks $\mathbf{1}_N$ and $\mathbf{2}_N$ is shown in (c) and (d), respectively. Intensity of peaks $\mathbf{2}_N$ is about 6 times larger than intensity of peaks$\mathbf{1}_N$. Microwave frequency 9.6734 GHz, magnetic field 339 mT, time τ =136 ns.

Table 1. Hyperfine couplings and quadrupole coupling constants for weakly coupled nitrogens in the environment nearest the Cu_A center estimated from HYSCORE spectra.

Sample	Frequencies	A, MHz	$K=e^2Qq/4h$, MHz	Assignment	Reference
WT-Cu_AAz	(3.1, 2.0)	0.68	0.35-0.40[a]	Remote N_ε H46, H120	This work
H120G-Cu_AAz	(2.9, 2.2) (3.5, 3.0)	0.43 0.39	0.37-0.43[a] 0.61-0.71[a]	Remote N_ε H46 Amide N	This work
COX, M160T9[e]	(2.8, 1.9) (4.1, 3.3)	0.51 0.80	0.35 (η=0.9)[b] 0.77 (η=0.88)[b]	Remote N, Im Amide N	29
COX, M160QT0[d]	(2.7; 2.0) (2.6; 2.2) (4.3, 3.1)	0.46 0.39 1.14	0.37-0.43[c] 0.36-0.42[c] 0.77 (η=0.76)[b]	Remote N, Im Amide N	29
COX M160ET0 pH 4.2	(2.8; 2.0) (2.8; 2.2)	0.36 0.46	0.38 (η=0.9)[b] 0.33 (η=0.9)[b]	Remote N, Im	29
COX M160ET0 pH 7.0	(2.7, 2.0) (2.7, 2.2)	0.32 0.42	0.37 (η=0.9)[b] 0.32 (η=0.9)[b]	Remote N, Im	29
N_2OR	(2.9, 1.9) (3.4, 2.5)	0.60 0.65	0.36 (η=0.7)[b] 0.58 (η=0.76)[b]	Remote N, Im Amide N	30

[a]estimated using Eq. 2; [b]estimated by spectral simulations, η is an asymmetry parameter of the nuclear quadrupole tensor;
[c]our estimate using Eq. 2; [d]M160T0 is the original soluble fragment construct of cyt ba_3 that encodes 135 amino acids of subunit II;

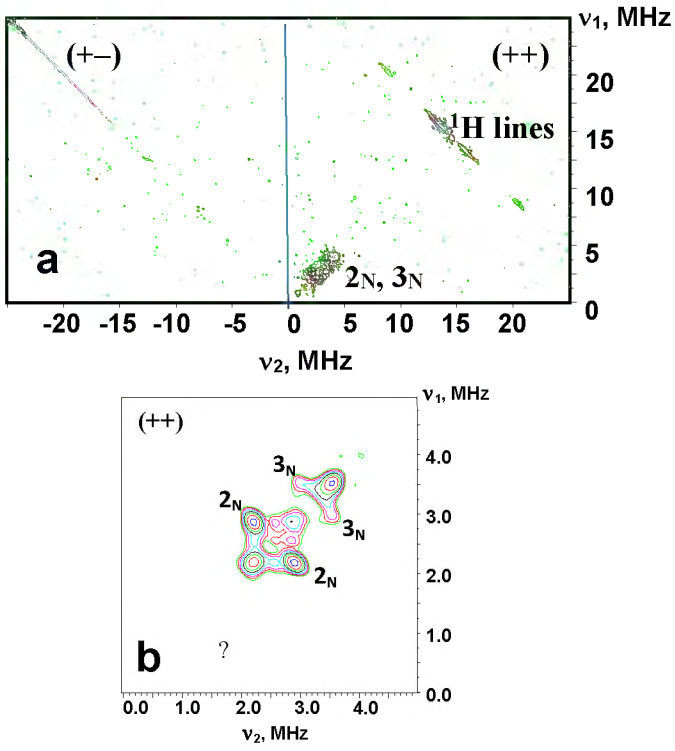

Figure 2. (++) and (+–) quadrants of the ^{1}H and ^{14}N HYSCORE spectrum of H120G-Cu_AAz showing (a) absence of cross-peaks $\mathbf{1}_N$ and location of cross-peaks $\mathbf{2}_N$ and $\mathbf{3}_N$ from weakly coupled nitrogens, and ^{1}H cross-ridges. Cross-peaks $\mathbf{2}_N$ and $\mathbf{3}_N$ at enhanced resolution are shown in (b). Microwave frequency 9.7018 GHz, magnetic field 339 mT, time τ =136 ns.

and expression for maximum value of $\nu_{dq\pm}$ (Eq. 2)[25]

$$A_N = \frac{\nu_{dq+}^2 - \nu_{dq-}^2}{8\nu_N} \qquad \text{(Eq. 2)}$$

where ν_N is the nuclear Zeeman frequency, A_N is the predominantly isotropic hyperfine coupling, $K=e^2qQ/4h$ is the quadrupole coupling constant, and η is the asymmetry parameter. In contrast, the similar HYSCORE spectrum for H120G-Cu_AAz does not show any cross-peaks in (+–) quadrant, which suggests the absence of the nitrogens with similar coupling of the order ~15 MHz and less (Figure 2a).

We attempted simulation of the $\mathbf{1}_N$ cross-peaks from coordinated histidine nitrogen shown in Figures 1a,c. This simulation matches the analysis performed quite well. Example of the simulations is shown in Figure S4 and additional details are described therein.

Weakly coupled nitrogens. In addition to cross-peaks $\mathbf{1}_N$ from the strongly coupled nitrogens, there are one pair of non-extended (ellipsoid shape) intensive cross-peaks $\mathbf{2}_N$ at (3.1, 1.98) MHz (~0.03 MHz) in the (++) quadrant of the WT-Cu_AAz HYSCORE spectrum located closely to the diagonal line, due to small difference in the correlated frequencies (Figure 1b,d). We interpret these cross-peaks as correlating to ν_{dq+} and ν_{dq-} transitions from opposite manifolds of weakly coupled ^{14}N nuclei. In this case an application of Eq. S2 for the $\nu_{dq\pm}$ frequencies gives an estimate of the hyperfine coupling A_N=0.68 MHz and the quadrupole coupling constant K = 0.35-0.4 MHz (for the asymmetry parameter varying within $0<\eta<1$). The value of $K = e^2qQ/4h$ ~ 0.35-0.4 MHz is typical for protonated imidazole nitrogens,[24,26] which allows us to assign peaks $\mathbf{2}_N$ to the remote N_ε imidazole nitrogen in His ligands of the Cu_A center. This assignment is also confirmed by the ratio of the estimated hyperfine coupling for this nitrogen 0.68 MHz to the hyperfine coupling of the coordinated nitrogen 15.3 MHz. This ratio is close to ~20, which is a typical value for coordinated and remote nitrogens of the imidazole rings ligated to metals (e.g., Cu(II), VO(II), Fe(II)) in previously reported complexes and clusters.[26-28] This similarity probably reflects analogous spin density distribution over the imidazole ring, which is controlled by the protonation state of the remote atom.

The HYSCORE spectrum of the Cu_A center in H120G-Cu_AAz (Figure 2) shows two pairs of cross-peaks $\mathbf{2}_N$ and $\mathbf{3}_N$ at (2.93, 2.23) MHz and (3.5, 3.0) MHz from weakly coupled nitrogens in the (++)

quadrant with substantially different K values (Table 1). One of them is close to the K characteristic of the protonated imidazole nitrogen, but the other larger K value is more consistent with K reported for peptide nitrogens (Table 1).[29,30] Both estimated hyperfine couplings for these nitrogens are smaller than the couplings assigned to imidazole N_ε in WT-Cu_AAz and have an order ~0.4 MHz.

Proton HYSCORE. Besides the nitrogens, HYSCORE spectra provide information about protons interacting with the electron spin of the Cu_A cluster (Figures 1-3 and S3). The ^{1}H spectrum for WT-Cu_AAz contains four pairs of resolved cross-features located symmetrically relative to the diagonal line with the hyperfine splittings ~2, 6, 11, and 19 MHz. They are designated $\mathbf{1_H}$, $\mathbf{2_H}$, $\mathbf{3_H}$, and $\mathbf{4_H}$, respectively. The cross-features are well separated and show clearly pronounced maxima. This type of the spectrum can be explained by the lineshape properties for the cross-correlations from nuclei with spin I=1/2. The narrowness of the cross-ridges extending along the antidiagonal line suggests that axial anisotropic hyperfine tensors may apply for the interacting protons. The ideal cross-peak shape in this case is an arc-type ridge between the points ($\nu_{\alpha\perp}$, $\nu_{\beta\perp}$) and ($\nu_{\alpha\|}$, $\nu_{\beta\|}$) located on the $|\nu_\alpha \pm \nu_\beta| = 2\nu_{1H}$ lines (where ν_{1H} is the proton Zeeman frequency at the applied magnetic field). However, HYSCORE intensity at points ($\nu_{\alpha\perp}$, $\nu_{\beta\perp}$) and ($\nu_{\alpha\|}$, $\nu_{\beta\|}$), corresponding to orientations of the magnetic field along the $A_\perp$ and $A_\|$ principal directions of the hyperfine tensor, is equal to zero and is significantly suppressed at orientations around the principal directions.[31] Therefore, in HYSCORE spectra, only the central part of the cross-ridge , which corresponds to orientations of the magnetic field substantially different from the principal directions, will possess observable intensity. In contrast, the maximum intensity is detected around $\nu_{\alpha\perp}$ and $\nu_{\beta\perp}$ frequencies of each contributing proton in ENDOR spectra.

In addition, the peak intensity in HYSCORE varies with τ as $\sin(\pi\nu_\alpha\tau)\sin(\pi\nu_\beta\tau)$, producing different attenuation and suppression of peaks as τ is changed. Previous W-band ^{1}H ENDOR study[20] reported the average anisotropic parameter T for C_β-H protons in different Cu_A centers within ~1.4-1.7 MHz. The length of the cross-ridge can be accurately described in the current case by $|\nu_{\alpha(\beta)\|} - \nu_{\alpha(\beta)\perp}| = 3T/2$ or 2~2.5 MHz. This interval is also effectively decreased by the suppression of the intensity near $\nu_{\alpha(\beta)\|}$ and $\nu_{\alpha(\beta)\perp}$ for each ridge. Therefore, the proton ridges observed in the spectra in Figure 3 have a length close to the predicted and are not split in several parts due to τ influence. This is confirmed by the linear regression analysis as well (see below). A spectrum measured with the selected τ=136 ns allows us to demonstrate observable cross-peaks from all protons simultaneously despite the differences in the relative intensity.

The contour lineshape of the cross-ridge from nuclear spin S=1/2 is described by equation (Eq. 3)[32]

$$\nu_1^2 = Q\nu_2^2 + G \qquad \text{(Eq. 3)}$$

where $Q = (T+2a-4\nu_{1H})/(T+2a+4\nu_{1H})$ and $G = [2\nu_{1H}(4\nu_{1H}^2 - a^2 + 2T^2 - aT)]/(T+2a+4\nu_{1H})$, a and T are isotropic and anisotropic components of the axial hyperfine tensor (a-T, a-T, a+$2T$), respectively.

Eq.3 defines a straight line segment in ν_1^2 *vs.* ν_2^2 coordinates.[32] This property allows us to test the identity of the features $\mathbf{1_H}$-$\mathbf{4_H}$ via the linear regression of their ridges in ν_1^2 vs. ν_2^2 coordinates. Linear regressions of the cross-ridges $\mathbf{1_H}$-$\mathbf{4_H}$ are shown in Figure S3. One can note that the points of all ridges are fitted along different and not coincident straight lines, indicating that they belong to the different protons.

Coefficients of the Q and G determined by the linear regressions define the isotropic and anisotropic components of the hyperfine tensors under an axial approximation for four different sources of protons (Table S1). Only three pairs of the cross-ridges with the splittings ~2, 12, and 20 MHz are observed in the ^{1}H HYSCORE spectrum of H120G-Cu_AAz. From the corresponding tensors shown in Table S2, one can see that the anisotropic couplings (T) for all protons are very close with the average value ~2.1±0.2 MHz. In contrast, the isotropic couplings (a) vary in a broad interval ~15 MHz.

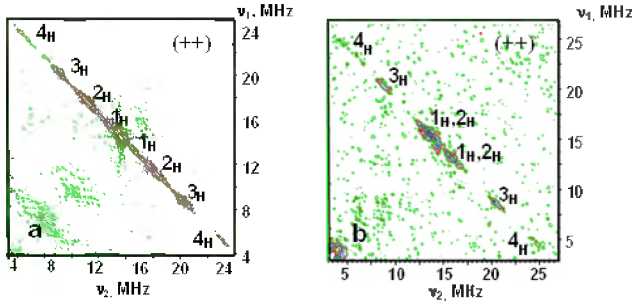

Figure 3. Contour presentation of ^{1}H HYSCORE spectra of Cu_AAz (a) and H120G Cu_AAz (b). Instrumental parameters are the same as in Figures 1 and 2. Hyperfine splittings reported in the text for both proteins are determined in first order as a difference $A=|\nu_1-\nu_2|$, where ν_1 and ν_2 are coordinates of the point with the maximum intensity for cross-peaks $\mathbf{1_H}$-$\mathbf{4_H}$.

■ DISCUSSION

Computational analysis of the valence delocalization in Cu_A center. In order to clarify the difference in the interpretations of the valence-delocalization by EPR and ENDOR described above, Xie *et al.* applied a series of spectroscopic techniques, including EPR, UV−vis, MCD, resonance Raman, and XAS to WT-Cu_AAz at high and low pH and His120Ala-Cu_AAz and correlated the results with DFT calculations.[33] EPR spectra at high and low pH display differences similar to those between WT-Cu_AAz and its H120 variants.[34] Two models of the Cu_A site associated with the protonation of one histidine ligand were used in DFT calculations. The first model is based on the highly symmetric Cu_2S_2 core with two His ligands. In the second model, His120 is protonated and replaced by a nearby H_2O ligand. DFT calculation shows that in both models, the Cu_A center is valence delocalized. The changes of the electron spin density at Cu and S atoms do not exceed 0.03.[33] However, an important difference between the two models is that the distorted ligand field produces ~0.01 4s mixing at Cu(H_2O) into the ground-state wave function of the binuclear site. This mixing decreases the isotropic contribution to the hyperfine tensor for one copper in the binuclear Cu center significantly (~3 times) and causes the collapse to a four-line hyperfine splitting pattern in the EPR spectra of the Cu_A center at low pH and in its His120 variants. The ability of Cu_A in azurin to remain valence-delocalized, even with the loss of a His ligand, is explained by the strong and direct Cu−Cu bond in the diamond core of Cu_A. Despite the DFT results[33] explaining the transformation of EPR spectra in Cu_A proteins, the conclusion about essentially identical ENDOR spectra for the WT-Cu_AAz and its variants[19] has required experimental evidence to quantitatively verify the DFT predicted, minor redistributions of the spin density in the Cu_A site. Below we discuss the support of our HYSCORE data for this previous computational analysis.

Strongly coupled nitrogens. The coupling $A_{N\perp}$ = 15.3 MHz derived from the HYSCORE spectrum of WT-Cu_AAz is in good agreement with the $A_{N\perp}$ values 13.6 MHz for Cu_A in N_2OR,[35] and 15.8 MHz, 15.5 MHz, 14.1 MHz in bovine heart cyt aa_3 and cyt caa_3 and ba_3 from *Thermus thermophilus*, respectively,[36] obtained from ENDOR experiments. The interval of couplings ~14-16 MHz is

about two times smaller than the $A_{N\perp}$ reported for different complexes of Cu^{2+} with nitrogen ligation (see, Table 2 in ref. 35). Based on these considerations, $A_{N\perp}$=15.3 MHz coupling can be assigned to the N_δ of the histidine ligands coordinated to the mixed valent Cu(+1.5)…Cu(+1.5) cluster. One can note that there are no indications of even poorly resolved splitting of cross-peaks $\mathbf{1_N}$ from strongly coupled nitrogens in the HYSCORE spectrum (Figure 1c), suggesting highly symmetrical distribution of the unpaired electron over the cluster, in line with a 7-component hyperfine structure from two coppers in the EPR spectrum.

The conclusion about similarity of Cu_A nitrogen couplings in the Cu_AAz and its H120N and H120G variants reported in the previous Q-band ENDOR study[19] was based on the observation of a common feature near 11 MHz assigned to a single-quantum transition of coordinated ^{14}N (Figure S7). It leads to an estimate of the four possible hyperfine couplings 14.1, 14.5, 15.1, and 16.7 MHz for $A_{N\perp}$. The value of 15.1 MHz is very close to $A_{N\perp}$ obtained from HYSCORE spectrum of the WT-Cu_AAz. However, our HYSCORE spectrum for H120G-Cu_AAz does not show any cross-peaks in the (+–) quadrant, which indicates an absence of nitrogens with similar coupling of the order ~15 MHz or smaller value (Figure 2). There is only one more example where the coupling of ~15 MHz was resolved in an X-band HYSCORE spectrum.[23] In that work, the reported HYSCORE spectra of the mixed-valent [Fe(II), Fe(III)] state of the binuclear cluster in methemerythrin, coordinated by five His ligands, shows (dq_+; dq_-) cross-peaks from four nitrogen couplings with $A_{N\perp}$ =5.0, 6.3, 9.4, and 15.3 MHz. The intensities of the cross-features consecutively decreased with the increase in $A_{N\perp}$. The observation of larger couplings was not reported in the literature to the best of our knowledge. These results suggest that even a slight increase of hyperfine coupling above ~15 MHz makes the dq-dq lines from coordinated nitrogens invisible in the X-band HYSCORE spectra. DFT calculations[33] for the two models described above predict an increase of spin density population, up to 0.04, on the coordinated nitrogen of His46 in H120 variants of Cu_AAz in comparison with the 0.03 in WT-Cu_AAz. The total increase of the spin population on copper and nitrogen is ~16%.[4,33] One can suggest that this increase in the spin density on the Cu-N(His46) fragment of H120G-Cu_AAz will elevate the hyperfine coupling A_N up to several MHz above 15 MHz causing it to be experimentally unobservable due to a decrease of the ESEEM intensity coefficient. The $\mathbf{1_N}$ cross-peaks would therefore vanish from the H120G-Cu_AAz's spectrum, as has been observed in other Cu_A systems.[29]

Previously HYSCORE spectra were only reported for the Cu_A center in a water soluble fragment of the cytochrome ba_3 subunit II of *Thermus thermophilus* (COX) and its Met160Gln and Met160Glu variants where methionine, the axial ligand to one of the coppers, was replaced by glutamic acid or glutamine.[13,29] These variants show changes in the g_z-region of the EPR spectra giving larger copper hyperfine splitting and better resolved 7-component spectra.[13] The effects of mutations were further studied by HYSCORE and ENDOR spectroscopy.[29] Experimental HYSCORE spectra provided in the study exhibit (0 – 6.0, -6.0 – 6.0) MHz frequency intervals along two axes with cross-features from weakly coupled nitrogens. The cross-peaks at high-frequencies in the (+–) quadrant, similar to the $\mathbf{1_N}$ features resolved in the Cu_AAz spectrum (Figure 1a,c), were not reported in that work. In contrast, the lines assigned to strongly coupled nitrogens with an estimated value of hyperfine coupling of ~13-17 MHz were observed in X- and W-band ENDOR spectra.[29] If the higher limit of this estimate corresponds to the actual coupling, then they would again be experimentally unobservable, thus explaining the absence of high-frequency cross-peaks in the (+-) quadrant of the X-band HYSCORE in this case.

Weakly coupled nitrogens. The HYSCORE spectrum of WT-Cu_AAz shows interactions with only one type of weakly coupled nitrogen, assigned to the N_ε of the His ligand based on the estimated quadrupole coupling constant K~0.4 MHz. While the two WT-Cu_AAz histidines appear to have overlapping hyperfine coupling constants of 15.3 MHz for the strongly coupled N_δ's, it is interesting to note that the weakly coupled N_ε's on the two histidines may have inequivalent coupling constants, which is not clearly resolved, but evident as a small shoulder oriented along the diagonal of features $\mathbf{2_N}$ (Figures 1b,d). The location of these shoulders is consistent with the peaks $\mathbf{2_N}$ position in the spectrum of the H120G-Cu_AAz variant. Feature $\mathbf{2_N}$ in H120G-Cu_AAz (Figure 2b) lacks any shoulder due to the presence of only one His Nε. Indeed two types of signals with minor differences between hyperfine couplings assigned to the Nε of histidine ligands were resolved in ^{14}N HYSCORE spectra of COX samples at different pHs[29] (Table 1). In addition, NMR measurements report difference in the spin delocalization on the protons of the His ligands of the Cu_A center in different proteins and particularly on the N_ε-H.[37] The reason for this difference could arise from the fact that one of the Nε's is more solvent exposed[38] than the other, and also that the two histidine ligands are tilted differently, with inequivalent bond angles, and bond distances. It would be possible for the Nδ's on two histidines to be coupled similarly with the copper ion, while the Nε's are not.

The spectrum of H120G-Cu_AAz exhibits the Nε interaction plus an additional nitrogen with larger K~0.7 MHz typical for peptide protein nitrogens. Resolution of this additional weak interaction can be attributed tentatively to a redistribution of the spin density between the cluster's atom and/or to structural changes near the cluster as a result of the mutation. Two types of weakly coupled nitrogens around the Cu_A center, also assigned to the remote nitrogen of the coordinated imidazole residue(s) and to a backbone peptide nitrogen, were found in the HYSCORE spectra of cytochrome ba_3 and methionine variants discussed above (Table 1).[29] Also, similar assignments of the weakly coupled nitrogens were performed for the Cu_A center in N_2OR[30] based on analysis of the three-pulse ESEEM frequencies. Results from these studies collected in Table 1 show similar values of the quadrupole coupling constant for each type of nitrogen, but the hyperfine couplings vary by two-fold, reflecting differences in the protein environment around the Cu_A site in each protein.

In addition, two more pairs of cross-peaks at (0.7, ~4.2) and (1.4, ~4.2) MHz were observed in the HYSCORE spectra of the COX proteins.[29] These features are typical for the remote nitrogen of the imidazole ligand bound to a localized Cu^{2+}, satisfying the cancelation condition $|\nu_{14N} - |A|/2| \sim 0$.[26] They belong to the ($\nu_{0,-}$, ν_{dq}) and (ν_+, ν_{dq}) correlations of the remote imidazole nitrogen(s) of the Type 2 copper center which is present in different amounts in all studied samples.[29] In addition, the appearance of similar features is expected if the unpaired electron in the Cu_A center of the H120G-Cu_AAz would be completely localized on the copper with coordinated His46. However, our spectra do not contain such cross-features, again supporting the spin delocalized structure. In addition, although the previous study with a Q-band rapid passage signal showed evidence for a minority component of mononuclear Type 2 copper in the variant sample,[19] our lack of cross-features (0.7, ~4.2) and (1.4, ~4.2) MHz indicates that our samples have only a small amount of T2 copper impurities.

Protons. The previous Q-band ENDOR study of WT-Cu_AAz and its H120N and H120G variants reported observation of lines with the splittings of ~6 MHz and ~12-13 MHz, which were absent in the corresponding spectra of the mononuclear copper complexes.[19]

They are close to two intermediate couplings ~6 and ~11 MHz (Figure 3) observed in our HYSCORE spectrum of WT-Cu_AAz. In contrast, the spectrum of H120G-Cu_AAz does not show the peaks $\mathbf{2_H}$ with 6 MHz splitting and the splitting of peaks $\mathbf{3_H}$ is slightly increased to 12 MHz.

The differences in HYSCORE spectra of WT- and H120G-Cu_AAz are qualitatively consistent with the Q-band ENDOR spectra from ref. 19. In these spectra (see Figure S5) the doublet with splitting ~6 MHz is clearly observed and well-separated from other lines in the spectrum of WT-Cu_AAz only. The intensity of this feature is significantly smaller in the spectra of H120G-Cu_AAz and looks like a shoulder of the more intense lines from weakly coupled protons. In agreement with these changes, we suggest that the 6 MHz splitting of peaks $\mathbf{2_H}$ is decreased and partially overlapped with the peaks $\mathbf{1_H}$ in the HYSCORE spectrum of H120G-Cu_AAz. The lineshapes of the doublets with the splitting ~12-13 MHz in Q-band ENDOR spectra are also different in the WT- and H120G-Cu_AAz, especially in the high-frequency component. It is broader in WT-Cu_AAz. In HYSCORE spectra the corresponding differences between the two proteins are manifested in a slight increase of $\mathbf{3_H}$ splitting.

The very weak lines $\mathbf{4_H}$ with the splitting ~19 MHz in HYSCORE spectra of both samples can be tentatively assigned to a mononuclear Type 2 copper complex, despite the lack of nitrogen cross-peaks (0.7, ~4.2) and (1.4, ~4.2) MHz expected for Cu^{2+}-imidazole complexes stated above. A doublet with a similar splitting ~20 MHz was observed in Q- and W-band ENDOR spectra of mononuclear complexes and not identified in Cu_A azurins.[19,20] In addition, most recent NMR and ENDOR studies of the Cβ protons in the Cu_A proteins discussed below have not reported so large a coupling. The relative intensity of the nitrogen and proton cross-peaks in HYSCORE spectra of T2 copper is not known and needs more detailed analysis.

Table 2. Reported isotropic hyperfine couplings (MHz) for Cβ protons of cysteine ligands in Cu_A center of different proteins.

Protein	a_1	a_2	a_3	a_4	Ref.
N_2OR	8.6	10.4	11.7	13.3	35
N_2OR	9.1	11.0	12.2	13.8	20
COX[a]	6.8	10.0	12.2	15.4	20
COX[b]	8.1	10.3	11.6	13.3	20
Cu_AAz	9.0		12.5		20
Cu_AAz	~6		~12.5		19
ba$_3$ oxidase[c]	4.33	8.9	9.53	10.5	37
M160Q *ba*$_3$ oxidase[c]	1.87	9.75		11.38	37
Cu_AAz	5.2 |7.6|[d]	10.8	|12.8|[d]		This work
H120G Cu_AAz			11.9	|13.9|[d]	This work

[a]The recombinant water-soluble fragment of subunit II of *Thermus thermophilus* cytochrome *c* oxidase (COX) *ba*$_3$ (M160T9), [b]its M160QT0 variant, where the weak axial methionine ligand has been replaced by a glutamine. [c]NMR study of the soluble subunit II of *Thermus thermophilus ba*$_3$ oxidase [d]Linear fitting analysis of the cross-ridges gives two possible solutions with opposite relative signs of *a* and *T* (see, Supporting Info Figure S3 and Tables S1 and S2).

More details in the proton couplings were explored in a comparative study of Cu_A centers in N_2OR, Cu_AAz, and COX *bo*$_3$ and its M160Q variant using X- and W-band ^{1}H ENDOR.[20] Two types of proton resonances are present in all spectra. The first group is attributed to the cysteine Cβ protons and contributes to the broad range of couplings 7-15 MHz. The second group includes the protons with weak couplings smaller than 3 MHz. Among all these proteins, Cu_AAz possesses the simplest orientation-selective ENDOR spectra from Cβ protons, consisting of a doublet of lines with the average splitting of ~10.8 MHz and width ~3 MHz. Using these characteristics, the maximum and minimum values of the isotropic coupling for Cβ protons were estimated to be 12.5 and 9 MHz, respectively. Similar lines in the spectra of other proteins studied in that work[20] exhibit more complex lineshapes with additional features that were used to distinguish the different protons. As a result, isotropic and anisotropic components of hyperfine tensors for all four Cβ protons were derived from the simulations of W-band spectra of N_2OR and two COX proteins. Currently available information about isotropic couplings with Cβ protons in the Cu_A proteins is summarized in Table 2.

Analysis of the isotropic couplings for Cβ protons in ref. 20 was performed using the expression $a_H = \rho_S(B\sin^2\phi + C)$ describing their dependence on the H-C-S-S dihedral angle, ϕ.[35] In this expression, B and C represent contribution from hyperconjugation and polarization, respectively, ρ_S and is the unpaired electron density on the Cys S atom. Previous studies[37] and the available crystallographic structures of the Cu_A centers indicate well conserved H-C-S-S dihedral angles. Minimum and maximum isotropic couplings for each Cu_A were assigned to protons with ϕ around 0° and 90° that provided a direct estimate of $\rho_S B$ and $\rho_S C$. Further, analysis of these parameters has established the variation of the ρ_S within the range ~0.15 - 0.25 in studied proteins with the minimum value in Cu_AAz.[20] However, this analysis was performed under the assumption of equal spin density on both sulfur atoms. NMR studies on native systems[14] and DFT calculations[33] for the models with two and one His ligand in Cu_AAz show a substantial difference of 0.19 and 0.25 between spin density population on two sulfurs in the case with two His ligands. The difference in spin populations decreases (0.21 and 0.23) in the H120 variant Cu_A with one His.

If we assign peaks $\mathbf{1_H}$ to weakly coupled protons and $\mathbf{4_H}$ to the mononuclear copper, then the remaining peaks $\mathbf{2_H}$ and $\mathbf{3_H}$ belongs to the Cβ protons in HYSCORE spectra of Cu_AAz samples. This analysis suggests that the lines from four Cβ protons partially overlap and produce only two resolved cross-peaks in X-band HYSCORE spectra. The largest component of the anisotropic hyperfine tensor for Cβ protons of Cu_A center in different proteins determined from W-band ENDOR spectra varies within 2.8 - 3.4 MHz.[20] The W-band ENDOR defines the average value of T~1.4-1.7 MHz that is smaller than T~2.2±0.2 MHz obtained from our analysis of the cross-peak lineshapes. The difference with ENDOR data likely arises from the overlap of the lines produced by different Cβ protons with close isotropic couplings in HYSCORE spectra. It increases the apparent length of the cross-ridges and leads to a larger anisotropic component in the formal analysis.

■ CONCLUSIONS

In this work, we have described a comparative study of the ^{1}H and ^{14}N hyperfine interactions for the Cu_A center in WT- and H120G-Cu_AAz using the two-dimensional ESEEM technique, HYSCORE.

Application of HYSCORE has identified clear differences between ^{14}N and ^{1}H hyperfine interactions in WT- and H120G-Cu_AAz. Specific findings include:

(i) The observation of the cross-peaks from histidine nitrogens directly coordinated to Cu_A with hyperfine coupling $A_{N\perp}$ =15.3 MHz

in WT-Cu_AAz. This is the first experimentally determined quantitative information about hyperfine interaction with coordinated nitrogens in Cu_AAz. In contrast, similar peaks were not observed in the spectra of H120G-Cu_AAz, which indicates an increased value of $A_{N\perp}$. We suggest that the increase would not need to be more than a few MHz, which is in line with the rise of the spin population of ~16% at Cu-N fragment in the variant. It would be sufficient enough for the cross-peaks to vanish in X-band HYSCORE.

(ii) The ^{14}N HYSCORE spectrum of WT-Cu_AAz resolves interaction with only one type of weakly coupled nitrogen, assigned to the remote N_ε of coordinated imidazole residues based on the quadrupole coupling constant K~0.4 MHz. The spectrum of H120G-Cu_AAz demonstrates this plus an additional feature typical for backbone peptide nitrogens with larger K~0.7 MHz.

(iii) The ^1H HYSCORE spectra exhibit an opposite shift of the cross-ridges of only ~1 MHz from C_β protons, consistent with the DFT predicted variation of the spin density ~0.02 (i.e. ~10%) on sulfur atoms of the Cu_A cluster in H120 variants relative to the wild-type protein.

These findings provide the first experimental support for the previous DFT analysis that predicted changes of the spin population ~0.02-0.03 on copper and sulfur atoms of the Cu_A center in H120 variants relative to the WT-Cu_AAz, and contribute to resolving the contradicting conclusions between EPR and ENDOR studies of valence distribution in Cu_AAz and its variants.[19]

We suggest that more detailed characterization of the spin density distribution is needed for the construction of an experimentally supported model of spin density distribution in Cu_A centers at different pH and in different variants. DFT calculations[33] discussed above were mostly focused on the hyperfine couplings from two coppers due to absence of any precisely characterized hyperfine couplings of the other magnetic nuclei. One can propose that copper couplings determined from the EPR spectra can be further supported by the hyperfine tensors of the coordinated nitrogens and of the C_β carbons of the cysteine ligands. Those can be obtained from ^{15}N ENDOR and ^{13}C HYSCORE experiments in a similar manner as that in refs. 35 and 39, respectively, for other systems. High-field ENDOR and ELDOR detected NMR can also be useful for this purpose.[40] These additional data would provide a more detailed view of the unpaired spin density distribution around the Cu_2S_2 molecular core for more extended DFT modeling.

ASSOCIATED CONTENT

Supporting Information

The Supporting Information is available free of charge on the ACS Publications website.
Field sweep pulsed EPR spectra, additional HYSCORE spectra of Cu_A in WT-Cu_AAz and H120G-Cu_AAz, equations for an estimate of hyperfine coupling from ^{14}N double-quantum frequencies, analysis of the ^1H HYSCORE spectra, and previously published Q-band ENDOR spectra (PDF).

AUTHOR INFORMATION

Corresponding Authors

*dikanov@illinois.edu

Present Addresses

#Department of Chemistry and Biochemistry
University of Minnesota Duluth
1039 University Dr.
Duluth, MN 55812

Author Contributions

The manuscript was written by contributions of all authors. All authors approve of the final version of the manuscript.

Notes

The authors declare no competing financial interests.

ACKNOWLEDGMENT

This investigation was supported in part by the DE-FG02-08ER15960 (S.A.D., pulsed EPR work) Grant from the Chemical Sciences, Geosciences and Biosciences Division, Office of Basic Energy Sciences, Office of Sciences, U.S. Department of Energy, and National Science Foundation CHE 17-10241 (Y.L., protein design and engineering).

REFERENCES

1. Yoshikawa, S.; Muramoto, K.; Shinzawa-Itoh, K.; Mochizuki, M. Structural studies on bovine heart cytochrome *c* oxidase. *Biochim. Biophys. Acta, Bioenerg.* **2012**, 1817, 579-589.
2. Carreira, C.; Pauleta, S. R.; Moura, I. The catalytic cycle of nitrous oxide reductase - The enzyme that catalyzes the last step of denitrification. *J. Inorg. Biochem.* **2017**, *177*, 423-434.
3. Pauleta, S. R.; Dell'Acqua, S.; Moura, I. Nitrous oxide reductase. *Coord. Chem. Rev.* **2013**, *257*, 332-349.
4. Wilson, T. D.; Yu, Y.; Lu, Y. Understanding copper-thiolate containing electron transfer centers by incorporation of unnatural amino acids and the Cu_A center into the type 1 copper protein azurin. *Coord. Chem. Rev.* **2013**, *257*, 260–276.
5. Liu, J.; Chakraborty, S.; Hosseinzadeh, P.; Yu, Y.; Tian,S.; Petrik, I.; Bhagi, A.; Lu,Y. Metalloproteins containing cytochrome, iron–sulfur, or copper redox centers. *Chem. Rev.* **2014**, *114*, 4366–4469.
6. Kroneck, P. M. H. Walking the seven lines: binuclear copper A in cytochrome c oxidase and nitrous oxide reductase. *JBIC J. Biol. Inorg. Chem.* **2018**, 23, 27–39.
7. Morgada, M. N.; Abriata, L. A.; Zitare, U.; Alvarez-Paggi, D.; Murgida, D. H.; Vila, A. J. Control of the electronic ground state on an electron-transfer copper site by second-sphere perturbations. *Angew. Chem., Int. Ed.* **2014**, *53*, 6188-6192.
8. Dennison, C.; Vijgenboom, E.; de Vries, S.; van der Oost, J.; Canters, G. W. Introduction of a Cu_A site into the blue copper protein amicyanin from *Thiobacillus versutus*. *FEBS Lett.* **1995**, *365*, 92-94.
9. van der Oost, J.; Lappalainen, P.; Musacchio, A.; Warne, A.; Lemieux, L.; Rumbley, J.; Gennis, R. B.; Aasa, R.; Pascher, T.; Malmström, B. G.; Saraste, M., Restoration of a lost metal-binding site: construction of two different copper sites into a subunit of the *E. coli* cytochrome *o* quinol oxidase complex. *EMBO J.* **1992**, *11*, 3209-3217.
10. Espinoza-Cara, A.; Zitare, U.; Alvarez-Paggi, D.; Klinke, S.; Otero, L.H.; Murgida, D. H.; Vila, A. J., Engineering a bifunctional copper site in the cupredoxin fold by loop-directed mutagenesis. *Chem. Sci.* **2018**, *9*, 6692-6702.
11. Hay, M.; Richards, J. H.; Lu, Y. Construction and characterization of an azurin analog for the purple copper site in cytochrome c oxidase. *Proc. Natl. Acad. Sci. U.S.A.* **1996**, *93*,461–464.
12. Robinson, H.; Ang, M. C.; Gao, Y.-G.; Hay, M. T.; Lu, Y.; Wang, A. H. J. Structural basis of electron transfer modulation in the purple Cu_A center. *Biochemistry* **1999**, *38*, 5677–5683.
13. Slutter, C. E.; Gromov, I.; Richards, J. H.; Pecht, I.; Goldfarb, D. Mutations of the weak axial ligand in the *Thermus* Cu_A center modulates its electronic structure. *J. Am. Chem. Soc.* **1999**, *121*, 5077-5078.
14. Abriata, L. A.; Ledesma, G. N.; Pierattelli, R.; Vila, A. J. Electronic structure of the ground and excited states of the Cu_A site by NMR spectroscopy. *J. Am. Chem. Soc.* **2009**, *131*, 1939-1946.
15. Abriata, L. A.; Alvarez-Paggi, D.; Ledesma, G. N.; Blackburn, N. J.; Vila, A. J.; Murgida, D. H. Alternative ground states enable pathway switching in biological electron transfer. *Proc. Natl. Acad. Sci. U. S. A.* **2012**, *109*, 17348-17353, S17348/1-S17348/23.

16. Ledesma, G. N.; Murgida, D. H.; Ly, H. K.; Wackerbarth, H.; Ulstrup, J.; Costa-Filho, A. J.; Vila, A. J. The met axial ligand determines the redox potential in Cu_A sites. *J. Am. Chem. Soc.* **2007**, *129*, 11884-11885.
17. Wang, X.; Berry, S. M.; Xia, Y.; Lu, Y. The role of histidine ligands in the structure of purple Cu_A azurin. *J. Am. Chem. Soc.* **1999**, *121*, 7449–7450.
18. Berry, S. M.; Wang, X.; Lu, Y. Ligand replacement study at the His 120 site of purple Cu_A azurin. *J. Inorg. Biochem.* **2000**, 78, 89–95.
19. Lukoyanov, D.; Berry, S. M.; Lu, Y.; Antholine, W. E.; Scholes, C. P. Role of the coordinating histidine in altering the mixed valency of Cu_A: An electron nuclear double resonance-electron paramagnetic resonance investigation. *Biophys. J.* **2002**, *82*, 2758-2766.
20. Epel, B.; Slutter, C. S.; Neese, F.; Kroneck, P. M. H.; Zumft, W. G.; Pecht, I.; Farver, O.; Lu, Y.; Goldfarb, D. Electron-mediating Cu_A centers in proteins: A comparative high field ^{1}H ENDOR study. *J. Am. Chem. Soc.* **2002**, *124*, 8152-8162.
21. Höfer, P.; Grupp, A.; Nebenführ, H.; Mehring, M. Hyperfine Sublevel Correlation (HYSCORE) spectrocopy: A 2D ESR investigation of the squaric acid radical. *Chem. Phys. Lett.* **1986**, *132*, 279−282.
22. Dikanov, S. A.; Xun, L.; Karpiel, A. B.; Tyryshkin, A. M.; Bowman, M. K. Orientationally-selected two-dimensional ESEEM spectroscopy of the Rieske-type iron-sulfur cluster in 2,4,5-trichlorophenoxyacetate monooxygenase from Burkholderia cepacia AC1100. *J. Am. Chem. Soc.* **1996**, *118*, 8408−8416.
23. Dikanov, S. A.; Davydov, R. M.; Graslund, A.; Bowman. M. K. Two-Dimensional ESEEM spectroscopy of nitrogen hyperfine couplings in methemerythrin and azidomethemerythrin. *J. Am. Chem. Soc.* **1998**, *120*, 6797-6805.
24. Dikanov, S. A.; Tyryshkin, A. M.; Hüttermann, J.; Bogumil, R.; Witzel, H. Characterisation of histidine coordination in VO^{2+} substituted D-xylose isomerase by orientationally-selected ESEEM spectroscopy. *J. Am. Chem. Soc.* **1995**, *117*, 4976-4986.
25. Dikanov, S. A., Tsvetkov, Yu. D., Bowman, M. K., and Astashkin, A. V. Parameters of quadrupole coupling of ^{14}N nuclei of chlorophyll *a* cations determined by electron spin echo method. *Chem. Phys. Lett.*, **1982**, *90*, 149-153.
26. Mims, W. B.; Peisach, J. The nuclear modulation effect in electron spin echo for complexes of Cu^{2+} and imidazole with ^{14}N and ^{15}N. *J. Chem. Phys.* **1978**, *69*, 4921−4930.
27. Dikanov, S. A.; Burgard, C.; Hüttermann, J. Determination of the hyperfine coupling with the remote nitrogen in the VO^{2+}-(imidazole)$_4$ complex by ESEEM spectroscopy. *Chem. Phys. Lett.* **1993**, *212*, 493-498.
28. Iwasaki, T.; Kounosu, A.; Uzawa, T.; Samoilova, R. I.; Dikanov, S. A. Orientation-selected ^{15}N-HYSCORE detection of weakly coupled nitrogens around the archaeal Rieske [2Fe-2S] center. *J. Am. Chem. Soc.* **2004**, *126*, 13902-13903.
29. Slutter, C. E.; Gromov, I.; Epel, B.; Pecht, I.; Richards, J. H.; Goldfarb, D. Pulsed EPR/ENDOR characterization of perturbations of the Cu_A center ground state by axial methionine ligand mutations. *J. Am. Chem. Soc.* **2001**, *123*, 5325-5336.
30. Jin, H.; Thomann, H.; Coyle, C. L.; Zumft, W. G. Copper coordination in nitrous oxide reductase from Pseudomonas stutzeri. *J. Am. Chem. Soc.* **1989**, *111*, 4262-4269.
31. Dikanov, S. A.; Tyryshkin, A. M.; Bowman, M. K. Intensity of cross-peaks in HYSCORE spectra of S=1/2, I=1/2 spin systems. *J. Magn. Reson.* **2000**, *144*, 228-242.
32. Dikanov, S. A.; Bowman, M. K. Cross-peak lineshape of two-dimensional ESEEM spectra in disordered S=1/2, I=1/2 spin system. *J. Magn. Reson., Ser. A* **1995**, *116*, 125-128.
33. Xie, X.; Gorelsky, S. I.; Sarangi, R.; Garner, D. K.; Hwang, H. J.; Hodgson, K. O.; Hedman, B.; Lu, Y.; Solomon, E. I. Perturbations to the geometric and electronic structure of the Cu_A site: Factors that influence delocalization and their contributions to electron transfer. *J. Am. Chem. Soc.* **2008**, *130*, 5194-5205.
34. Hwang, H. J.; Lu, Y. pH-dependent transition between delocalized and trapped valence states of a Cu_A center and its possible role in proton-coupled electron transfer. *Proc. Natl. Acad. Sci. U.S.A.* **2004**, *101*, 12842–12847.
35. Neese, F.; Kappl, R.; Hüttermann, J.; Zumft, W. G.; Kroneck, P. M. H. Probing the ground state of the purple mixed valence Cu_A center in nitrous oxide reductase: a CW ENDOR (X-band) study of the ^{65}Cu, ^{15}N-histidine labeled enzyme and interpretation of hyperfine couplings by molecular orbital calculations. *J. Biol. Inorg. Chem.* **1998**, *3*, 53–67.
36. Gurbiel, R. J.; Fann, Y. C.; Surerus, K. K.; Werst, M. M.; Musser, S. M.; Doan, P.; Chan, S. I.; Fee, J. A.; Hoffman, B. M. Detection of two histidyl ligands to Cu_A of cytochrome oxidase by 35-GHz ENDOR: ^{14,15}N and ^{63,65}Cu ENDOR studies of the Cu_A Site in bovine heart cytochrome aa_3 and cytochromes caa_3 and ba_3 from *Thermus thermophilus*. *J. Am. Chem. Soc.* **1993**, *115*,10888–10894.
37. Fernandez, C. O.; Cricco, J. A.; Slutter, C. E.; Richards, J. H.; Gray, H. B.; Vila, A. J. Axial ligand modulation of the electronic structures of binuclear copper sites: Analysis of paramagnetic ^{1}H NMR spectra of Met160Gln Cu_A. *J. Am. Chem. Soc.* **2001**, *123*, 11678-11685.
38. Salgado, J.; Warmerdam, G.; Bubacco, L.; Canters, G. W. Understanding the electronic properties of the Cu_A site from the soluble domain of cytochrome *c* oxidase through paramagnetic ^{1}H NMR. *Biochemistry* **1998**, *37*, 7378–7389.
39. Taguchi, A.T.; Miyajima-Nakano, Y.; Fukazawa, R.; Lin, M.T.; Baldansuren, A.; Gennis, R. B.; Hasegawa, K.; Kumasaka, T.; Dikanov, S. A.; Iwasaki, T. Unpaired electron spin density distribution across reduced [2Fe-2S] cluster ligands by $^{13}C_\beta$-cysteine labeling. *Inorg. Chem.* **2018**, *57*, 741−746.
40. Cox.N.; Nalepa, N.; Lubitz, W.; Savitsky, A. ELDOR-detected NMR: A general and robust method for electron-nuclear hyperfine spectroscopy? *J. Magn. Reson.* **2017**, 280, 63-78.

For Table of Contents Only

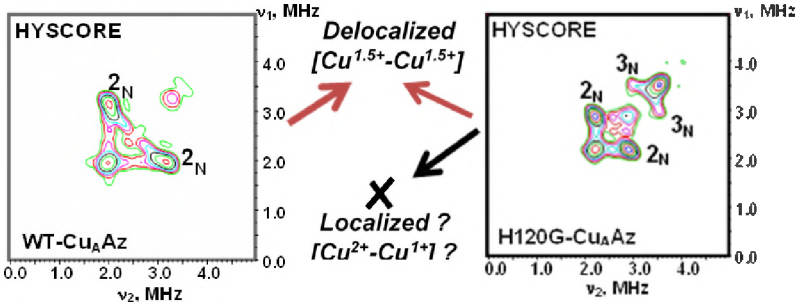

The two-dimensional HYSCORE spectroscopy has identified clear differences between ^{14}N and ^{1}H hyperfine interactions in an engineered Cu_A center in azurin and its His120Gly variant. These findings provide the first experimental support for the DFT predicted minor changes of the spin population ~0.02-0.03 (i.e. ~10%) on copper and sulfur atoms of the Cu_A in H120 variants relative to the azurin and contribute in the development of quantitatively verified model of valence distribution in these proteins.